Orientational Distribution Function in Nematic Tobacco-Mosaic-Virus Liquid Crystals Measured by X-Ray Diffraction

R. Oldenbourg,[1] X. Wen,[1] R. B. Meyer,[1] and D. L. D. Caspar[1,2]

[1]*The Martin Fisher School of Physics, Brandeis University, Waltham, Massachusetts 02254*

[2]*The Rosenstiel Basic Medical Sciences Research Center, Brandeis University, Waltham, Massachusetts 02254*

(Received 6 July 1988)

Orientational distributions of the rod-shaped tobacco-mosaic-virus particle in magnetically aligned nematic solutions (0.05*M* borate buffer, *p*H 8.5) were measured by analysis of the angular spread of x-ray diffraction patterns. We measured Gaussian orientational distributions with order parameters varying between 0.77 in a solution with coexisting nematic and isotropic phase, to 0.95 in the single-phase nematic solution at higher concentration. Our experimental results are in good agreement with model calculations based on a modified Onsager theory for suspensions of hard rods.

PACS numbers: 61.30.Gd, 61.10.−i, 61.30.Eb, 64.70.Md

Aqueous suspensions of the tobacco mosaic virus (TMV) are regarded as an ideal model system of hard rods interacting via a screened Coulomb potential. Onsager developed the first theoretical model[1] for the isotropic-to-nematic phase transition in suspensions of long rods. The ordering was described by an anisotropic orientational distribution function of the rods which tends to be parallel to a common axis in the nematic suspension. In this Letter we present measurements of the ordering of TMV particles to test Onsager's theory. We have measured the particles' orientational distribution function by analyzing the angular spread of the equatorial x-ray diffraction from magnetically aligned nematic solutions of TMV. Previous studies of anisotropic x-ray scattering from thermotropic[2] and lyotropic[3] liquid crystals have measured the degree of orientational order by the evaluation of the arcing of diffraction features arising from interference effects between different particles. Furthermore, the angular spread of diffraction patterns of low-molecular-weight liquid crystals is greatly affected by the finite width of the diffraction features of the single molecule. In contrast, the intrinsic width of the equatorial layer line of the TMV diffraction pattern is much narrower than the highly collimated x-ray beams used to measure the scattering[4]; furthermore, interparticle interference effects are confined to very small scattering angles, so the independent-particle scattering can easily be measured to high resolution. Therefore, the angular spread of our diffraction patterns can be interpreted directly in terms of the orientational distribution of the rods in the nematic phase. Our analysis can be applied to other polymer liquid crystals and ordered phases of highly anisotropic particles.

Monodisperse stock solutions of the 300-nm-long TMV particles in 0.05*M* borate buffer, *p*H 8.5, were prepared by Cahoon according to procedures described elsewhere.[5] Stock solutions were checked for particle composition by ultracentrifuge analysis[6] and were found to be monodisperse. Nematic TMV suspensions were obtained by the dilution of stock solutions with the same buffer. In the sample with an average concentration of 0.116 g/cm^3, a birefringent phase settled out in equilibrium with an isotropic top phase (volume ratio $V_{\text{isotropic}}/V_{\text{nematic}}=0.71$). TMV concentrations were measured by uv absorption using a specific extinction coefficient of $OD_{\text{sp}}=3.06$ cm^3/mg (Ref. 6). Nematic specimens for x-ray diffraction measurements were oriented in thin-walled cylindrical quartz capillaries (diameter 0.7 mm, length about 8 cm) which were sealed with wax and stored in a vertical position.[7]

We exposed nematic TMV suspensions to a magnetic field of 2 T, which induces a uniform alignment of the nematic ordering parallel to the magnetic field.[8] The findings of the magnetic alignment and the polarizing microscope study are reported elsewhere.[9] Birefringences Δn of uniformly aligned samples were measured with a Berek compensator in the light path of the microscope (see Table I). Using the nematic order parameter S, measured by x-ray diffraction experiments presented below, we obtained the specific birefringence Δn_{sp} of nematic TMV suspensions: $\Delta n_{\text{sp}}=\Delta n/Sc$

TABLE I. Measured values of the TMV concentration c, the birefringence Δn, the order parameter S, and the width α of the Gaussian orientational distribution [Eq. (2)] of nematic TMV suspensions with 0.05*M* borate buffer, *p*H 8.5.

Sample No.	c (g/cm^3)	Δn (10^{-3})	S	α (radian)
1(iso)	0.106	...	...	...
1(nem)	0.123	1.84	0.77	0.261
2	0.124	1.97	0.82	0.233
3	0.150	2.66	0.91	0.170
4	0.151	2.70	0.92	0.159
5	0.161	2.92	0.94	0.135
6	0.162	2.90	0.92	0.157
7	0.173	3.20	0.95	0.124

$=1.94\times10^{-2}$ cm^3/g.

The sample capillary with a permanent magnet was mounted on a small-angle x-ray camera consisting of a double-mirror focusing system which provided a highly collimated, intense x-ray beam from an Elliott rotating anode x-ray generator with a Cu target.[10] The beam had a cross section of about 200×200 μm^2 and was focused on the film plane located 380 mm behind the sample. The guard slits were set such that diffraction into angles larger than 0.16° were free of parasitic background scattering. The angular width of the beam was 0.06°. X-ray diffraction patterns of nematic TMV suspensions were recorded on several films, which were either stacked in sequence or exposed separately for different time spans, to obtain a large dynamic range of the intensity measurements. Subsequently the optical density of each film was scanned with a 50-μm raster, and the density readings were corrected for film sensitivity, saturation effects, and film background[11] and converted to a two-dimensional array of intensity data.

The small-angle diffraction patterns of magnetically aligned, nematic TMV suspensions showed two intensity maxima at Bragg angles $\Theta\cong0.15°$ and 0.43° (see Fig. 1). The radial position of the maximum at $\Theta\simeq0.15°$ shifted to larger Bragg angles with increasing TMV concentration, while the position of the subsidiary maximum at $\Theta=0.43°$ was independent of TMV concentration. We checked for the presence of interparticle interference effects in the subsidiary maximum by computing the single-particle scattering function using a cylindrical shell model for the TMV particle.[12–14] The computed scattering function fitted exactly the intensity distribution in the subsidiary maximum of the recorded diffraction patterns, indicating that this maximum was the superposition of intramolecular scattering of TMV.

The angular spread of the maxima increased considerably with decreasing TMV concentration because of increased particle disorientation. A single TMV particle scatters x rays into a thin line of angular width $\lambda/(L\sin\omega)$, L being the length of the rod and ω the angle between the rod axis and the x-ray beam (x-ray wavelength $\lambda=0.154$ nm). With the range of values for ω in our specimens and $L=300$ nm, the linewidth is smaller than the angular width of the x-ray beam. The superposition of the scattering of rods with a continuous orientational distribution leads to a spread of the total intensity into concentric arcs. $G(\Psi)$ is the intensity distribution along an arc described by the angle Ψ from the equator (see Fig. 1). We find the following integral equation relating $G(\Psi)$ with the orientational distribution $f(\Gamma)$ of the rods:

$$G(\Psi)\cong\int I_s(\omega)f(\Gamma)\sin\omega\,d\omega\,. \tag{1}$$

$I_s(\omega)$ is the single-rod scattering intensity, which is proportional to $1/\sin\omega$. $f(\Gamma)$ is the probability density of finding a rod axis tilted at an angle Γ with respect to the mean axis of the nematic ordering. With the nematic mean axis perpendicular to the x-ray beam, the angles Ψ, Γ, and ω are geometrically related by[15] $\cos\Gamma=\cos\Psi\sin\omega$.

The integral equation (1) cannot be solved analytically for $f(\Gamma)$. As a trial function we have assumed $f(\Gamma)$ to be a Gaussian:

$$f(\Gamma)=A\exp[-\sin^2(\Gamma)/2\alpha^2]\,. \tag{2}$$

The substitution of (2) in Eq. (1) and our fitting the integral expression with two adjustable parameters (A and α) to the measured intensity distributions gave us excellent agreement with the experimental data (see Fig. 2). Values of the width α obtained by the fitting procedure are listed in Table I.

We note that for small enough α the following expan-

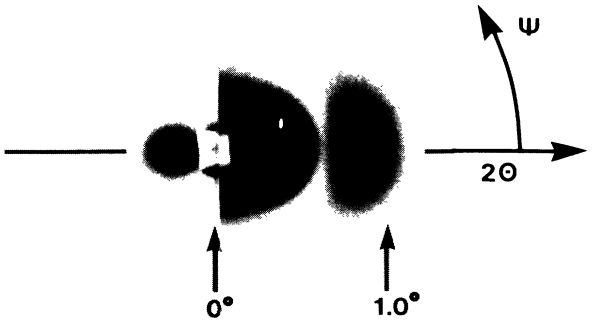

FIG. 1. Small-angle x-ray-diffraction patterns from magnetically aligned, nematic phase of sample No. 1; left: short-time exposure, right: 20 times longer exposure time.

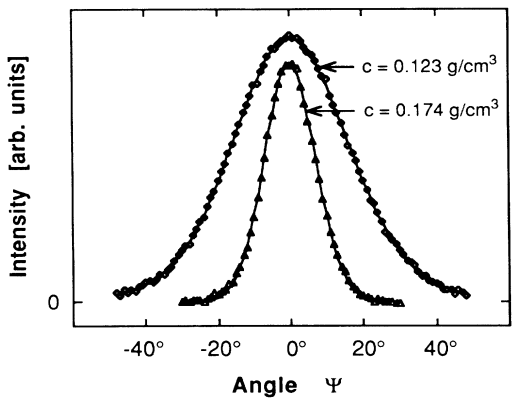

FIG. 2. The angular intensity distribution of the subsidiary maximum. Data sets for the least and most concentrated samples are shown. A datum point is the intensity integrated in a sector with the angular width $\Delta\Psi=1°$ and extending in the radial direction between $\Theta=0.32°$ and 0.64°. The continuous lines represent the best fit of the integral equation (1) with expression (2). The instrumental resolution is about $\Delta\Psi=1°$, which was estimated from the width of the central beam and the radial position of the second maximum.

sion for Eq. (1) with the Gaussian orientational distribution (2) can be found:

$$G(\Psi)=C'\exp(-\sin^2\Psi/2\alpha'^2)[1/\cos\Psi+\alpha'^2/2\cos^3\Psi+\cdots]. \quad (3)$$

We also adjusted expression (3) to the measured intensity distribution using the first term in the expansion series only. The best fit was only slightly worse than for the full integral expression and the width α' was higher than α by about 1%.

Values of the nematic order parameter S listed in Table I were obtained from the orientational distribution $f(\Gamma)$ with use of the definition[16]

$$S=\int f(\Gamma)[\tfrac{1}{2}(3\cos^2\Gamma-1)]d\Gamma.$$

Nematic TMV suspensions were uniaxially aligned by the application of a magnetic field. From observations made with the polarizing microscope[9] we concluded that defects in the alignment remained only in a thin layer close to the container walls. The thickness of that layer is about equal to one magnetic coherence length.[16] We estimated the magnetic coherence length to be 3 μm, using the reported values of the critical fields of the twist and splay Frederiks transitions in a nematic TMV sample[5] and the diamagnetic anisotropy of the single TMV particle[17] ($\Delta\chi_0=2.3\times10^{-24}$ J T^{-2}). Therefore, the fraction of the sample in the misaligned layer was negligibly small. Conversely, the suppression of long-wavelength orientation fluctuations by the magnetic field[16] produces only a negligible increase in the order parameter.[18]

The measured intensity distribution function $G(\Psi)$ was well fitted by the Gaussian orientational distribution of the rods in the nematic phase. Using Onsager's theory[1] for the ordering of very long rods (aspect ratio =length/diameter ≥ 25) Lee and Meyer[19] have found a numerical solution for $f(\Gamma)$ which is somewhat more peaked than the Gaussian distribution. Lee[20] introduced a scaling concept to extend Onsager's theory to smaller aspect ratios and found that the numerical solution for $f(\Gamma)$ for particles with smaller aspect ratios comes closer to a Gaussian distribution.[21]

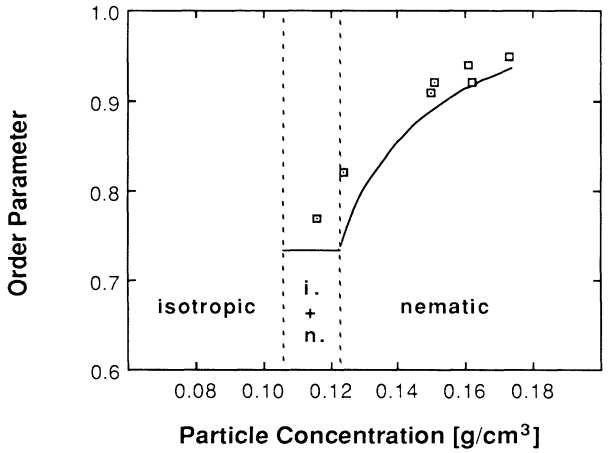

FIG. 3. Order parameters of nematic suspensions vs TMV concentration. The sample with an average TMV concentration of 0.116 g/cm^3 separated into an isotropic and a nematic phase with TMV concentrations indicated by the vertical lines. The continuous line was computed with a hard-rod model (Refs. 20 and 21).

The charges on the surface of the TMV particles increase the effective diameter of the rods.[1,19,22] We estimated the effective diameter by equating the volume fraction of TMV in the nematic phase of sample No. 1 with the critical volume fraction obtained by Lee[20] for systems of hard spherocylinders with finite length. The volume fraction of TMV was derived from the TMV number density, multiplied by the volume of a spherocylinder representing one TMV particle. The length of the spherocylinder including the radii of the hemispheres at each end was assumed to be close to the 300 nm length of the particle and its diameter was adjusted self-consistently until the experimental and theoretical volume fractions were equal. The hard-rod diameter was found to be 21.4 nm for TMV in 0.05M borate buffer, pH 8.5, corresponding to an axial ratio of 14.3. Hence, we estimated that the effective radius of the TMV rod is larger than the bare radius of the protein shell by about 1.7 nm, which is close to the Debye screening length of 1.4 nm.

In Fig. 3 the measured increase of the order parameter with increasing TMV concentration in the nematic phase is compared with the predicted increase of the order parameter[21] in the system of hard spherocylinders with the dimensions given above. The measured order parameters are comparable to those of Onsager's theory (0.79 at the phase transition), and larger than the simple, hard-rod theory predicts, indicating that the hard-rod model may not be quite an adequate representation of the interaction between particles with a soft repulsive potential. Furthermore, the hard-rod theory takes only the two-particle excluded volume into account, neglecting the higher-order terms in the viral expansion. Our samples possibly contain small amounts of end-to-end aggregated TMV particles (undetected by sedimentation analysis[6]), which could also increase the order parameter.[23,24]

Recently, structural phase transitions in systems of hard rods have been analyzed by computer simulations,[25] which can also be used to determine the angular distribution of rods interacting by repulsive potentials. The simulations provide the possibility for exploring the effects of soft or hard repulsive potentials, leading to useful comparisons with theory and experiments such as these.

This research was supported by the National Science Foundation through Grant No. DMR-8803582 awarded to R.B.M. and by Public Health Service Grant No. CA 47439 from the National Cancer Institute awarded to D.L.D.C.

[1]L. Onsager, Ann. N.Y. Acad. Sci. **51**, 627 (1949).

[2]A. J. Leadbetter, in *The Molecular Physics of Liquid Crystals,* edited by G. R. Luckhurst and G. W. Gray (Academic, London, 1979).

[3]N. S. Murthy, J. R. Knox, and E. T. Samulski, J. Chem. Phys. **65**, 4835–4839 (1976).

[4]J. D. Bernal and I. Fankuchen, J. Gen. Physiol. **25**, 111 (1941).

[5]S. Fraden, A. J. Hurd, R. B. Meyer, M. Cahoon, and D. L. D. Caspar, J. Phys. (Paris), Colloq. **46**, C3-85 (1985).

[6]H. Boedtker and N. S. Simmons, J. Am. Chem. Soc. **80**, 2550 (1958).

[7]J. Gregory and K. C. Holmes, J. Mol. Biol. **13**, 796 (1965).

[8]T. A. Cross, S. J. Opella, G. Stubbs, and D. L. D. Caspar, J. Mol. Biol. **170**, 1037 (1983).

[9]R. Oldenbourg and W. C. Phillips, Rev. Sci. Instrum. **57**, 2362 (1986).

[10]W. C. Phillips and I. Rayment, in *Methods in Enzymology,* edited by H. W. Wyckoff, C. H. W. Hirs, and S. N. Timasheff (Academic, New York, 1982), Vol. 114.

[11]W. C. Phillips and G. N. Phillips, Jr., J. Appl. Cryst. **18**, 3 (1985).

[12]We are grateful to D. Schneider, Brookhaven National Laboratory, for a computer program which is based on a Bessel function expansion of the Fourier transform of cylindrically symmetric particles.

[13]D. L. D. Caspar, Nature (London) **177**, 928 (1956).

[14]K. Namba and G. J. Stubbs, Acta Crystallogr. Sect. A **41**, 252 (1985).

[15]General studies of the effect of disorientation on the diffraction of fibrous materials were published by K. C. Holmes and J. Barrington Leigh, Acta Crystallogr. Sect. A **30**, 635 (1974), G. J. Stubbs, Acta Crystallogr. Sect. A **30**, 639 (1974), and L. Makowski, J. Appl. Crystallogr. **11**, 273 (1978).

[16]P. G. de Gennes, *The Physics of Liquid Crystals* (Clarendon, Oxford, 1975).

[17]P. Photinos, C. Rosenblatt, T. M. Schuster, and A. Saupe, J. Chem. Phys. **87**, 6740 (1987).

[18]The birefringence of nematic TMV increases by less than 1% in a magnetic field of 1 T. (S. Fraden, private communication.)

[19]S.-D. Lee and R. B. Meyer, J. Chem. Phys. **84**, 3443 (1986).

[20]S.-D. Lee, J. Chem. Phys. **87**, 4972 (1987).

[21]We thank Sin-Doo Lee for making his numerical results available to us.

[22]A. Stroobants, H. N. W. Lekkerkerker, and Th. Odijk, Macromolecules **19**, 2232 (1986).

[23]G. Oster, J. Gen. Physiol. **33**, 445 (1950).

[24]H. N. W. Lekkerkerker, Ph. Coulon, and R. Van Der Haegen, J. Chem. Phys. **80**, 3427 (1984).

[25]D. Frenkel, H. N. W. Lekkerkerker, and A. Stroobants, Nature (London) **332**, 822 (1988).

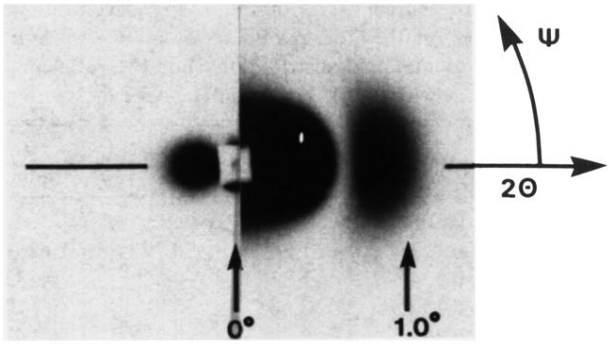

FIG. 1. Small-angle x-ray-diffraction patterns from magnetically aligned, nematic phase of sample No. 1; left: short-time exposure, right: 20 times longer exposure time.